THE CONDUCTIVITY OF LOW CONCENTRATIONS OF CO_2 DISSOLVED IN ULTRAPURE WATER FROM 0-100°C

Truman S. Light, Elizabeth A. Kingman, and Anthony C. Bevilacqua
Thornton Associates, Inc.
1432 Main Street
Waltham, MA 02154

Paper presented at the 209th American Chemical Society National Meeting, Anaheim, CA, April 2-6, 1995

ABSTRACT

The detection of ionic impurities in water is critical for several industries where there are stringent regulatory and industrial requirements. The most common instrumentation to measure low-level ionic impurities in ultrapure water systems is on-line conductivity/resistivity. This method is industry-tested in the identification of trace ionic contaminants, where the addition of 1 ppb of NaCl increases the conductivity of water from 0.055 to 0.057 μS/cm at 25.0°C. This difference is readily measurable with today's instrumentation. However, exposure of ultrapure water to air increases the water conductivity to ~0.8-1.5 μS/cm, depending on the actual atmospheric CO_2 concentration.

To advance our understanding of the CO_2-H_2O conductivity system, we have measured the conductivity of solutions of ultrapure water exposed to several low concentrations of CO_2 and we find that the conductivity varies by ~50% from 0-60°C with a maximum at ~45°C, whereas the conductivity of CO_2-free ultrapure water increases steadily by >2000% over the same range. We have independently compiled a model based on known physical properties of dissolved $CO_{2(aq)}$ to numerically predict the conductivity of ultrapure water as a function of temperature and CO_2 concentration in the presence of known atmospheric levels of CO_2 from 0-100°C. Our preliminary data demonstrate excellent agreement between the model and the experimental results. The conductivity measurement can also be used to detect trace CO_2 contamination in "ultrapure" gases as low as 0.050 ppm.

I. INTRODUCTION

Conductivity measurements are often employed to determine the impurity content of water due to its exposure to natural atmospheric components, especially carbon dioxide, CO_2. When testing for acidity in rain and other natural waters that result from SO_x and NO_x emissions, it is necessary to take into account the "natural acidity of water" due to CO_2 exposure so that the contaminating acid content is not overestimated. In the pharmaceutical, semiconductor, food/beverage, and power generation industries, pure water is often exposed to air (and CO_2), thereby increasing its conductivity and giving the appearance of a contaminant in the water. New standards put forth in U.S. Pharmacopeial Convention XXIII confirm that conductivities greater than that of pure water are permissible for "air-exposed" samples, if the only ionic impurity is naturally-occurring CO_2.

In ultrapure water, dissolved CO_2 from the atmosphere causes increased conductivity and decreased pH relative to the expected values of 0.0550 μS/cm and 7.00 pH at 25°C. For example, the conductivity of ultrapure water increases to approximately 1 μS/cm and the pH is lowered to 5.7 when water is exposed to air with a CO_2 content of 0.033%, a typical value for pure air. The other primary components of air do not form ionic species and do not affect the water conductivity.

In order to distinguish $CO_{2(aq)}$ in ultrapure water from contamination due to metallic or salt impurities, an accurate numerical model of the effect of dissolved CO_2 in water is desirable. For the most accurate model, the parameters for this model include : concentration of CO_2 in the ambient, Henry's Law constant, dissociation equilibria, ion mobilities, and water vapor pressure - each of which are temperature dependent. We present experimental data for the conductivity of water at typical CO_2 atmospheric concentrations from 0-75°C, and a model to numerically predict the conductivity from 0-100°C.

II. EXPERIMENTAL

A. Chemicals and Reagents

Ultrapure, de-ionized water (18.18 MΩ-cm at 25°C) was obtained from a closed-loop, re-circulating hot water system which includes 4 nuclear grade mixed-bed ion-exchange cartridges and a titanium-lined heater. Water was pumped from the storage tank, through the ion-exchange cartridges, through the heater, into the measurement apparatus, through a cooling loop, and back to the storage tank. The water was cooled prior to de-ionization to prevent degradation of the ion-exchange resin. Certified standard concentrations of CO_2 in N_2 were obtained from Scott Specialties Gases at 1010 ppm, 501 ppm, 299 ppm, and 20.4 ppm. The blank gas was 99.9995% N_2. Gas flow through the conductivity sensor was regulated and constant at 5 psia and 2 scfh.

B. Conductivity Apparatus and Instrumentation

The conductivity measurements were made in a 250 mL capacity chamber, shown in Figure 1, made of polyvinylidene fluoride (PVDF) with Teflon (FEP) fittings and valves, Viton o-rings, and a fritted-glass gas-dispersion tube. The top of the chamber had an opening to vent off gases. A stainless steel conductivity sensor (Thornton Associates sanitary sensor) was calibrated in the same water loop to a compensated resistivity of 18.18 MΩ-cm; the cell constant was determined to be 0.1005 cm^{-1}. The sensor was inserted in an inverted position in the chamber, sealed, and the chamber was immersed in a constant temperature bath that could be varied from 0-75°C. The conductivity cell sensor had a calibrated 1000 Ω platinum RTD embedded in it to measure temperature. A conductivity meter (Thornton Associates 770PC) was employed with its output being directed to a PC and stored to disk. The meter displayed the temperature, compensated conductivity, and uncompensated conductivity.

C. Procedure

De-ionized water at an elevated temperature was admitted to the conductivity apparatus and flushed until pure water was established in the apparatus (>18 MΩ-cm, <0.0555 μS/cm, compensated). The apparatus was sealed and $CO_{2(g)}$ was sparged through the cell continuously at constant pressure and flow rate. Data was collected and stored every 20 seconds as the temperature was varied.

FIGURE 1 : THE APPARATUS

CO_2 TEST CHAMBER

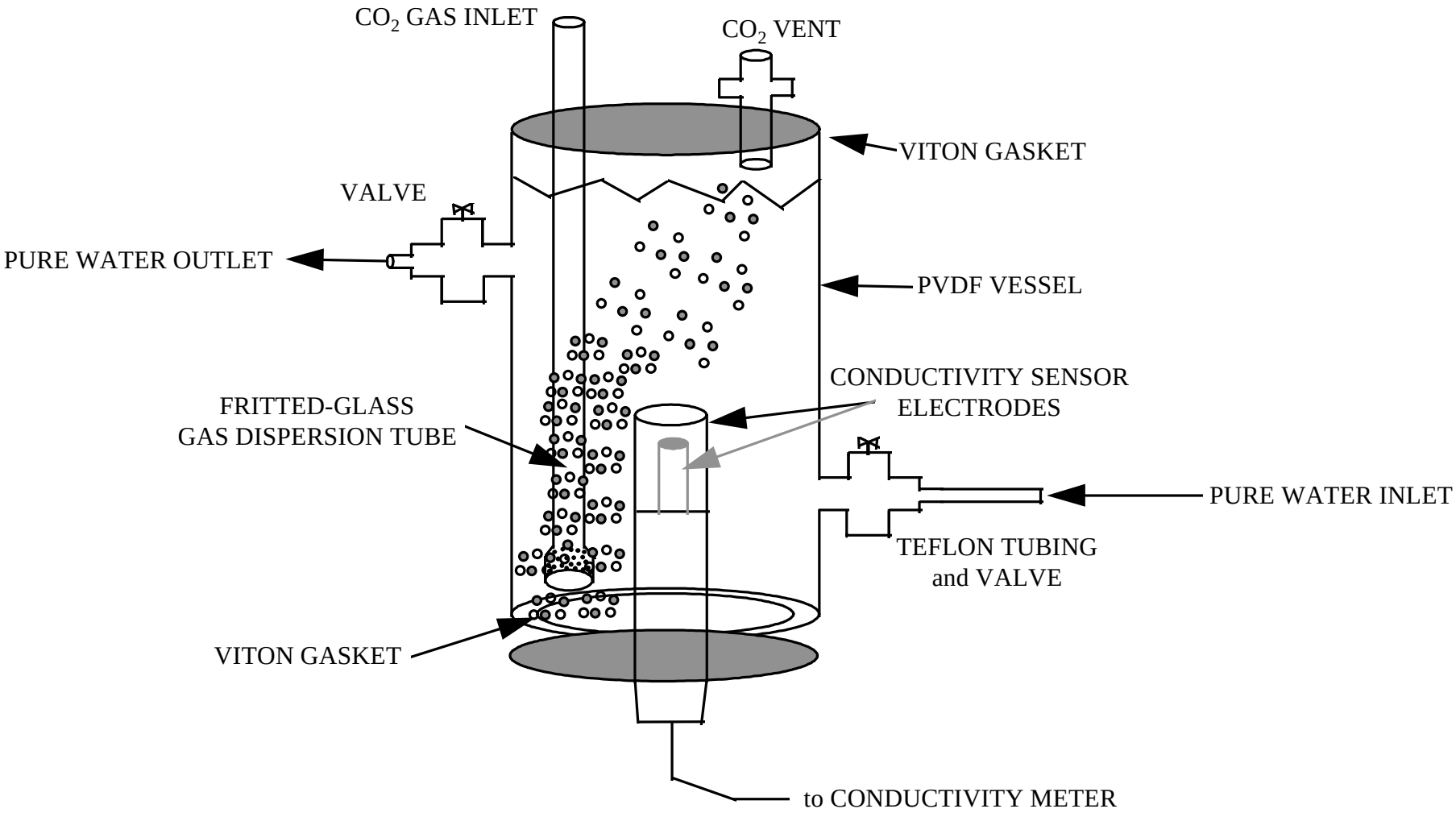

III. CONDUCTIVITY AS A MEASUREMENT METHOD

Advantages

Sensitive to ~0.1 ppb of salts
Inexpensive equipment
Easy to use
No cost to operate
Fast calibration
Reliable
Designed for on-line, real-time response
No sample handling or contamination

Disadvantages

Not ion-selective

The conductivity of an ionic solution is determined by :

$$K = 10^{-3} \cdot \sum_{i}^{\substack{all \\ ions}} \Lambda_i^{\circ} C_i \qquad \text{Eq. (1)}$$

where K is the conductivity (S/cm), $\Lambda°_i$ is the molar conductivity (S-cm^2/mole) of ion i at infinite dilution, and C_i is the concentration (mole/L) of ion i. In aqueous solutions, $\Lambda°_i$ can vary from 40 to 100 S-cm^2/mole for most simple ions, except H^+ (350) and OH^- (200) at 25°C, with a nominal temperature dependence of ~2.2%/°C. The temperature dependence for $\Lambda°_{H^+}$ and $\Lambda°_{OH^-}$ are well known and provided in the table below.

Only knowledge of the temperature and the components of the chemical system is required to predict the conductivity.

IV. MODEL

CO_2 reacts with water to form H_2CO_3, which is unstable and subsequently dissociates according to :

$$CO_{2(aq)} + H_2O \leftrightarrow (H_2CO_3) \leftrightarrow H^+ + HCO_3^- \qquad K_1 = 4.32 \times 10^{-7} \text{ at } 25°C \qquad \text{Eq.(2)}$$

H^+ and HCO_3^- are formed in roughly equal amounts, and these ions are the source of the large increase in conductivity upon exposure of pure water to air. The dissociation of HCO_3^- ($K_2 = 4.69 \times 10^{-11}$ at 25°C) does not contribute to the conductivity appreciably.

For the case of ultrapure water that is exposed to CO_2, the explicit conductivity equation becomes :

$$k = 10^{-3} \cdot \left(\Lambda^{\circ}_{H^+}[H^+] + \Lambda^{\circ}_{OH^-}[OH^-] + \Lambda^{\circ}_{HCO_3^-}[HCO_3^-] + \Lambda^{\circ}_{CO_3^{2-}}[CO_3^{2-}] \right) \qquad \text{Eq. (3)}$$

For ultrapure water that is exposed to a known quantity of $CO_{2(g)}$, the conductivity can be predicted by determining all 8 variables in Eq. 3 from known chemical and physical properties. However, by virtue of being a weak acid, the ion concentrations are not necessarily linear with $[CO_{2(aq)}]$. Also, the temperature dependence of each variable in Eq. 3 must be determined

A. Liquid-Vapor Equilibria

$[CO_{2(aq)}]$ dissolved in water is proportional to the partial pressure of CO_2 according to Henry's Law :

$$[CO_{2(aq)}] = K_h \times P_{CO_2(g)} \qquad \text{Eq. (4)}$$

where K_h is Henry's Law constant. $[CO_{2(aq)}]$ was determined from existing solubility data from 0-50°C at 1 atm total pressure. After $P_{CO_2(g)}$ was corrected for the vapor pressure of water at each temperature, K_h was determined. Since gases are not soluble at the boiling point of water, K_h is known to be 0 mol/L-atm at 100°C.

The values of K_h from 0-100°C were determined by fitting the existing data, including the 100°C data point, to a 5th order polynomial and allowing no more than one inflection point from 50-100°C.
P_{CO_2} is determined from

$$P_{CO_2} = \chi_{CO_2} \times P_{local} \qquad \text{Eq. (5)}$$

where P_{local} is the local barometric pressure, typically 1 atm, and χ_{CO_2}, the mole fraction of CO_2, is determined from

$$c_{CO_2} = \frac{P_{CO_2}}{P_{total}} = \frac{10^{-6} \cdot b \cdot P_{inlet}}{P_{inlet} + P_{H_2O}} \qquad \text{Eq. (6)}$$

where P_{inlet} is the tank delivery pressure, P_{H_2O} is the water vapor pressure, and β is the concentration (ppm) of CO_2 in nitrogen. From Eqs. 4-6, $[CO_{2(aq)}]$ is determined as a function of temperature and ambient CO_2 concentration.

B. Chemical equilibria and ion concentrations

Once $[CO_{2(aq)}]$ is determined, the ion concentration of each ion is determined from charge balance equations.

$$\left[H^+\right] = \frac{K_w}{\left[H^+\right]} + \frac{K_1\left[CO_{2(aq)}\right]}{\left[H^+\right]} + \frac{2K_1K_2\left[CO_{2(aq)}\right]}{\left[H^+\right]^2} \approx \sqrt{K_w + \left[CO_{2(aq)}\right]K_1} \qquad \text{Eq. (7)}$$

$$[OH^-] = K_w/[H^+] \qquad [HCO_3^-] = [H^+] - [OH^-] - 2 \times [CO_3^{2-}] \approx [H^+] - [OH^-] \qquad [CO_3^{2-}] \approx 0 \qquad \text{Eq. (7a)}$$

The temperature dependence of K_w is well known, but the temperature dependence of K_1 has only been reported from 0-50°C. Data could not be extrapolated beyond 50°C due to the non-linear behavior of K_1 at 0-50°C, so K_1 was indirectly determined by using the van't Hoff equation :

$$\frac{\partial \ln K_1}{\partial (1/T)} = -\frac{\Delta H_1}{R} \qquad \text{Eq. (8)}$$

ΔH_1 was determined as a function of temperature from a plot of ln K_1 vs. 1/T (K). A plot of ΔH_1 at 5°C intervals reveals a linear decrease vs. temperature (Figure 2). A linear least-squares (LLSQ) regression of ΔH_1 vs. T permitted us to obtain a linear temperature-dependent expression for ΔH_1 up to 100°C.

Figure 2. Determination of DH from van't Hoff Equation

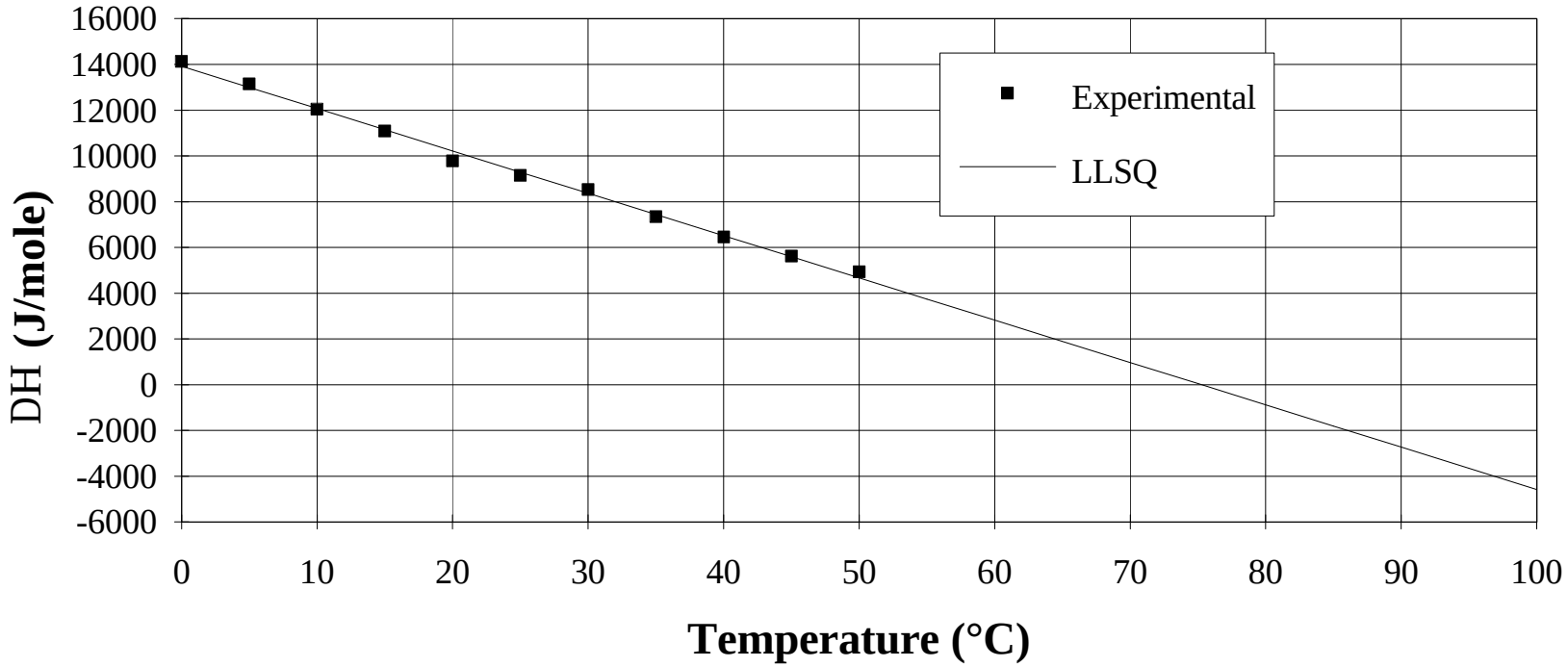

With values of ΔH_1 up to 100°C available, Equation 8 was integrated, new values of K_1 were obtained to 100°C (Figure 3), and a polynomial expression was derived for the K_1 (Table 1).

Figure 3. K_1 for Carbonic Acid

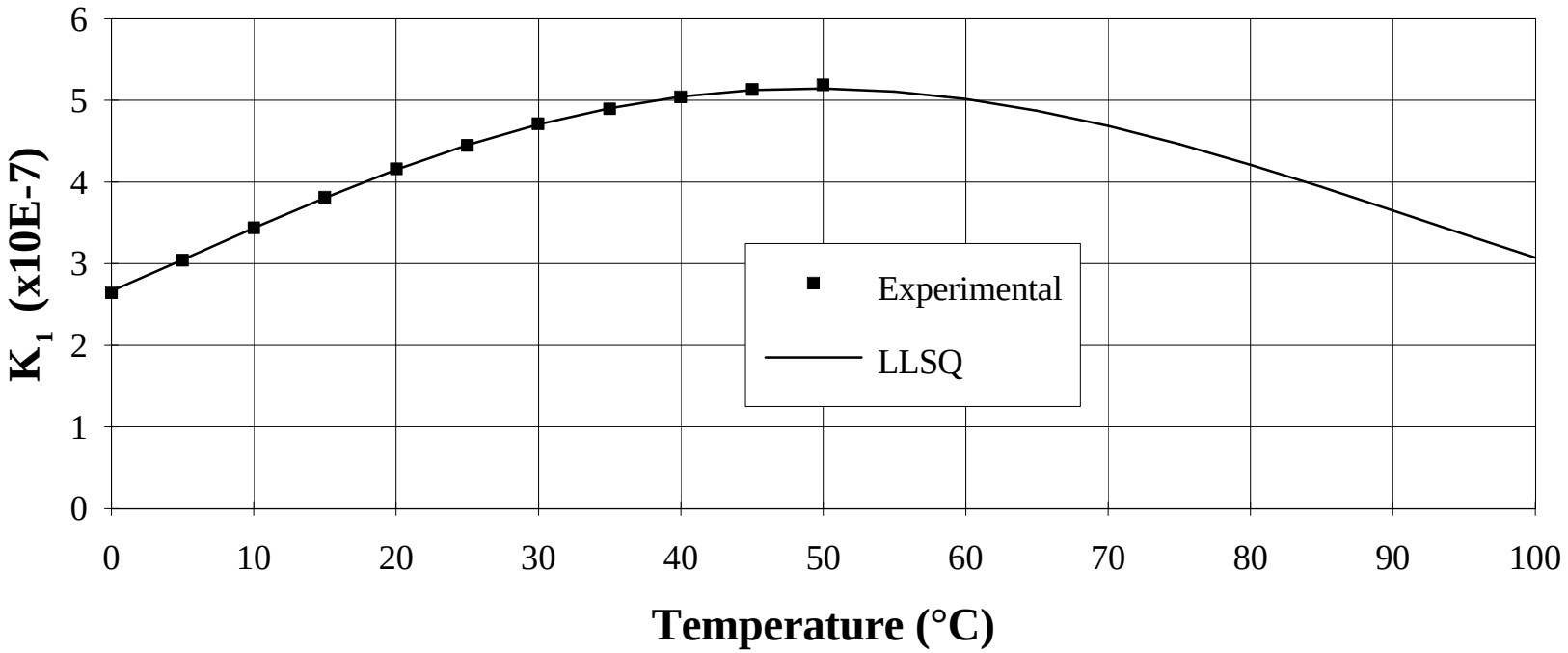

There are 6 species of interest: P_{CO_2}, $[CO_{2(aq)}]$, $[H^+]$, $[OH^-]$, $[HCO_3^-]$, and $[CO_3^{2-}]$. Once $P_{CO_2(g)}$ is known from Eqs. 4-6, the concentration of all other species may be determined from Eqs. 7-7a. Since $K_2 <<< K_1$, then $[HCO_3^-] >>> [CO_3^{2-}]$, thus the third term in Eq. 7 is negligible compared to the first two terms.

V. DISCUSSION

A. 0-45°C Experimental Data

An example of the raw data collected is shown in Figure 4 with the ambient CO_2 concentration at 20.4, 299, 498, and 1010 ppm. At the lowest temperatures (<5°C), the conductivity of pure water is less than 0.02 μS/cm (>50MΩ-cm). However, the exposure of 300-1000 ppm of CO_2 increases the conductivity of ultrapure water ~35-fold. As the temperature increases to ~45°C, the conductivity continues to increase by 50%. However, for pure water, the conductivity increase is >700%.

The increase in the conductivity with temperature of *carbonated* solutions is due to the usual causes : an increase in ion mobility and the increase in a K_w, resulting in more $[H^+]$. The other reason for the increase is due to the increase in K_1, resulting in a greater proportion of $[H^+]$ and $[HCO_3^-]$ relative to $[CO_{2(aq)}]$. The extent of the increase is countered by the decrease in $[CO_{2(aq)}]$ resulting from decreased solubility.

B. 45-80°C Temperature Experimental Data

At temperatures from 45-80°C, the conductivity of the 300-1000 ppm solutions decreases, resulting in a 10-30% loss in conductivity. Over the same temperature range, the conductivity of ultrapure water increases by >450%. This is contradictory behavior, despite increasing ion mobilities and K_w, resulting from the decreasing solubility of the CO_2. A minor secondary effect is also present as the proportion of $[H^+]$ and $[HCO_3^-]$ relative to $[CO_{2(g)}]$ also decreases as a result of K_1 decreasing with temperature.

C. Validity of the Model

There are nine temperature-dependent, fundamental constants used in Eqs. 3-8 that are needed to solve Eq. 3. They are $\Lambda°$ for the 4 ions, K_w, K_1 (and ΔH_1), K_2, K_h, and P_{H_2O}. Some of these constants are found in the literature from 0-100°C; others are available in the 0-50°C range and have been recently re-investigated, estimated, calculated, or interpolated beyond this range. We have already described our derivation for K_h and K_1 at elevated temperatures. K_2 has no impact on the conductivity for acidic conditions and K_w and P_{H_2O} are

well-known across the range. $\Lambda°_{HCO_3^-}$ and $\Lambda°_{CO_3^{2-}}$ are known at low temperatures and estimated at higher temperatures using +2.2%/°C. We have recently redetermined $\Lambda°_{H^+}$ and $\Lambda°_{OH^-}$ at high temperatures by re-measuring the conductivity of hot, ultrapure water.

Using the above parameters to create the model, we have compared the predicted conductivity for several ambient CO_2 concentrations to the data that we have collected in our lab (see Figure 4). We find excellent agreement between our results and the model at concentrations from 300-1000 ppm. Differences do not exceed 1% at 300 and 1000 ppm, and increase to 5% at 500 ppm, though given the agreement at 300 and 1000 ppm, we suspect the accuracy of the tank concentration. Data collected at 20.4 ppm exhibited greater differences from our model. Predicted conductivities for selected CO_2 concentrations from 0 to 2000 ppm are also provided in Figure 5.

D. Conductivity vs. pH

Figure 6 shows the pH of CO_2 solutions as a function of temperature, at selected concentrations, as calculated from Eq. 7. However, the low ionic activity of these solutions render the pH measurement difficult to make. In addition, the pH varies by only 0.3 pH units over the analytically useful range of 300 to 1000 ppm CO_2. This narrow range makes pH unsuitable for a useful analytical determination of CO_2 concentration. If the pH is beyond this range, then there is indication of an acidic or alkaline gas as an interferent.

At 25°C, the difference in the pH at 300 and 1000 ppm is ~17 mV at 25°C, or about 10× the noise level of a typical pH system. The conductivity difference at the same concentrations is 0.25 μS/cm, or ~100× the noise level in a typical industrial conductivity system.

E. Potential Applications

Potential applications derived from this study include the following : 1) the determination of CO_2 as an impurity in pure gases or air and 2) the determination of ionic impurities in water other than those due to CO_2. We were able to detect the difference in the impurity CO_2 level for different purity grades of nitrogen. For example, we took ultrapure water from our test loop and its exposure to the atmosphere increased its conductivity to ~1 μS/cm. Bubbling 99.99% N_2 (maximum 100 ppm contaminants) through the same sample would lower the conductivity to 0.2 μS/cm which is the equivalent of 20 ppm CO_2 in the ambient. After bubbling the same sample with 99.9995% N_2 (maximum 5 ppm contaminants), the conductivity lowered to 0.07-0.08 μS/cm, the equivalent of 1-2 ppm CO_2 in the ambient. Both sets of data are consistent with the manufacturers' purity specifications. At these concentrations, this measurement method is also feasible for the determination of the CO_2 content in air. We note that the use of a polyethylene or PVDF container yielded lower conductivities than a Pyrex beaker, presumably because of ions leaching from the glass.

The sensitivity of the conductivity of ultrapure water to dissolved CO_2 can also be used for the detection of trace levels of CO_2 in ultra high-purity (UHP) gases. By bubbling a UHP gas through ultrapure water, one can detect trace levels of CO_2 down to 0.050 ppm (>99.999995%). Other potential applications are the use of the conductivity measurement as a measure of degasification efficiency.

VI. CONCLUSIONS

We have created a temperature- and concentration-dependent model of the conductivity for water exposed to atmospheric levels (and beyond) of CO_2. We have also extended the knowledge of Henry's Law constant and the first acid dissociation constant for CO_2 in H_2O at temperatures above 50°C where data has not been available. We have experimentally verified this model over a range of relevant CO_2 and temperatures.

Figure 4. Experimental (---) vs. Predicted Conductivity

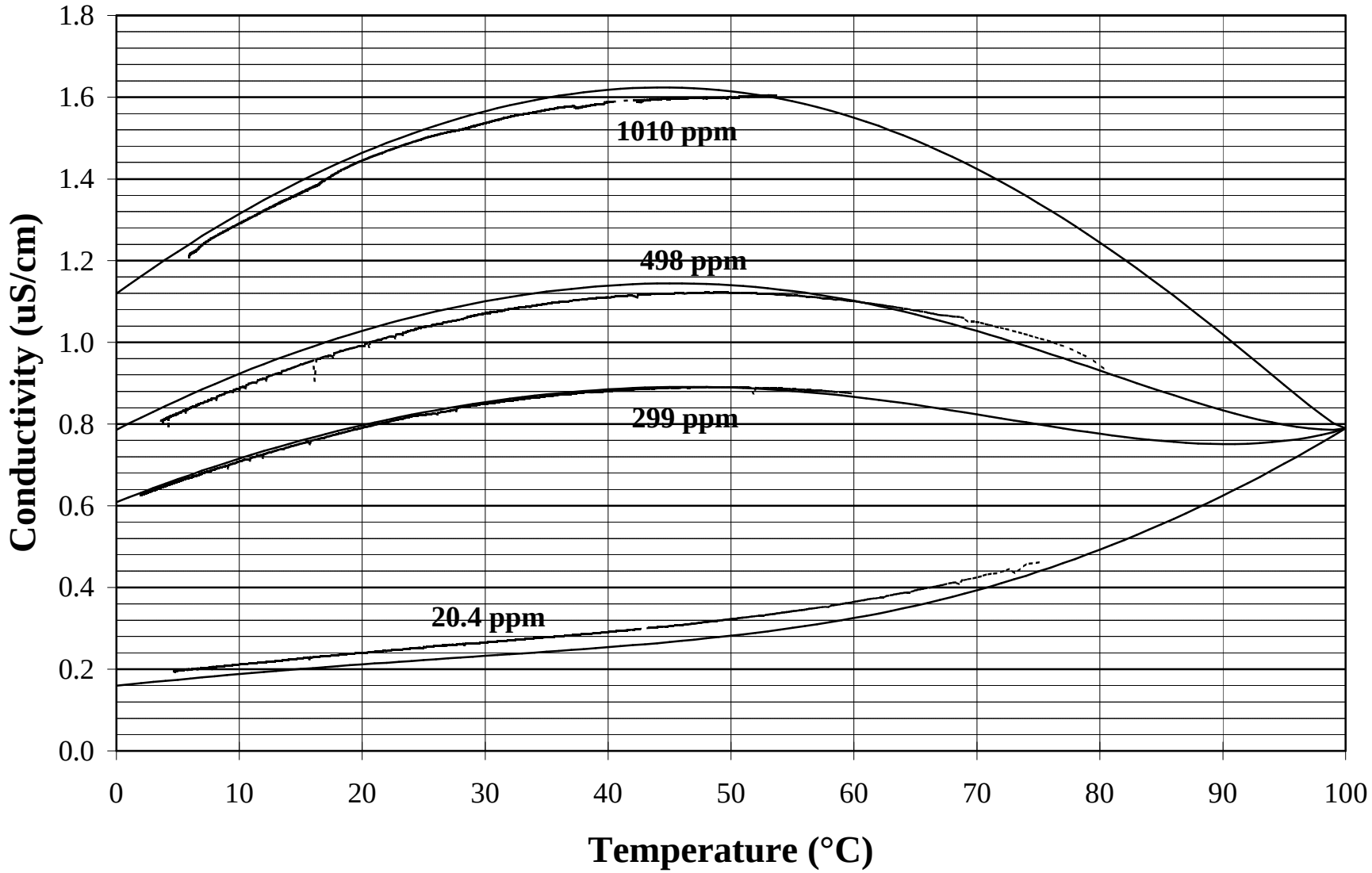

Figure 5. Predicted Conductivity for Various [CO2(g)]

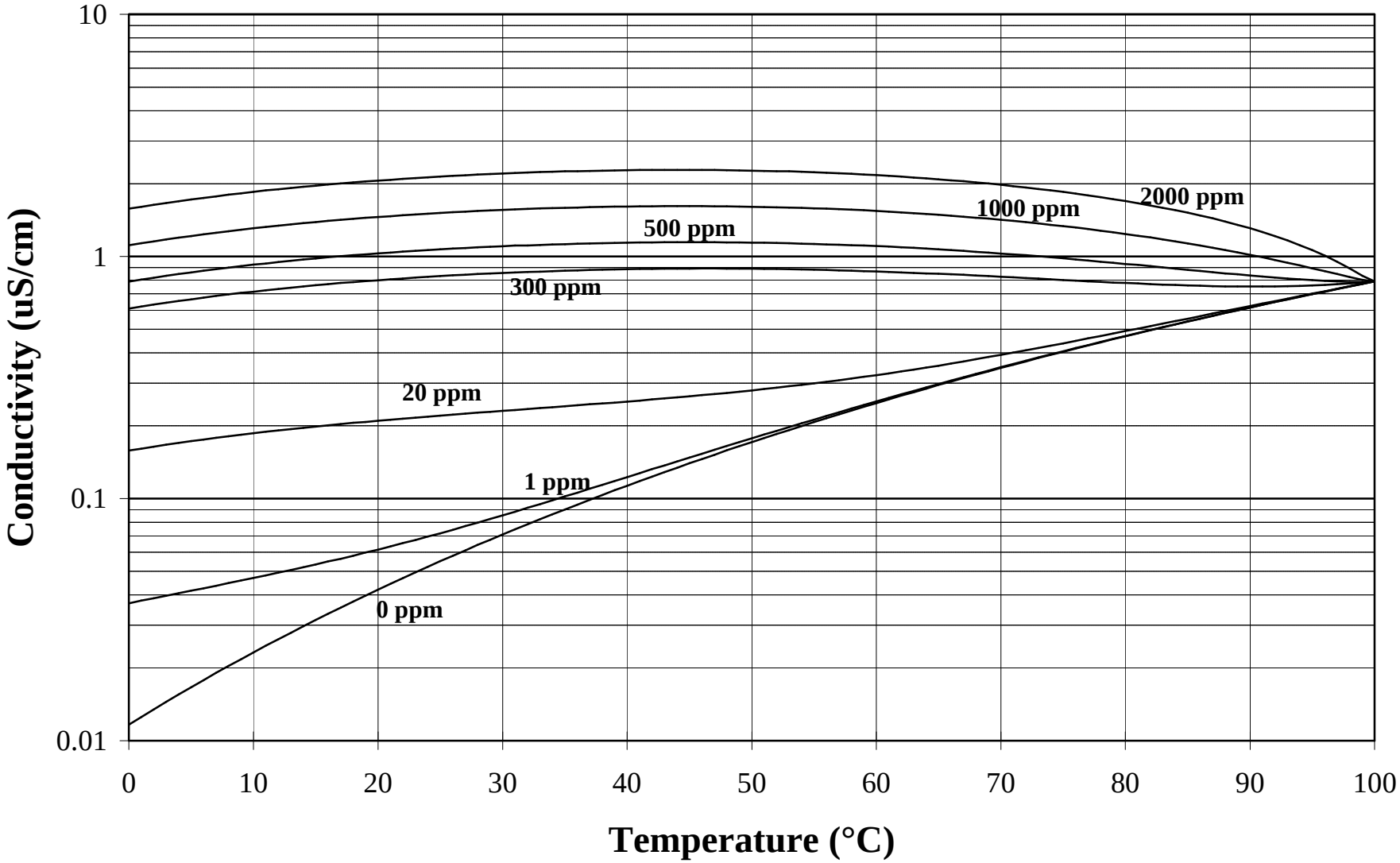

Figure 6. Predicted pH of CO2 in Ultrapure Water

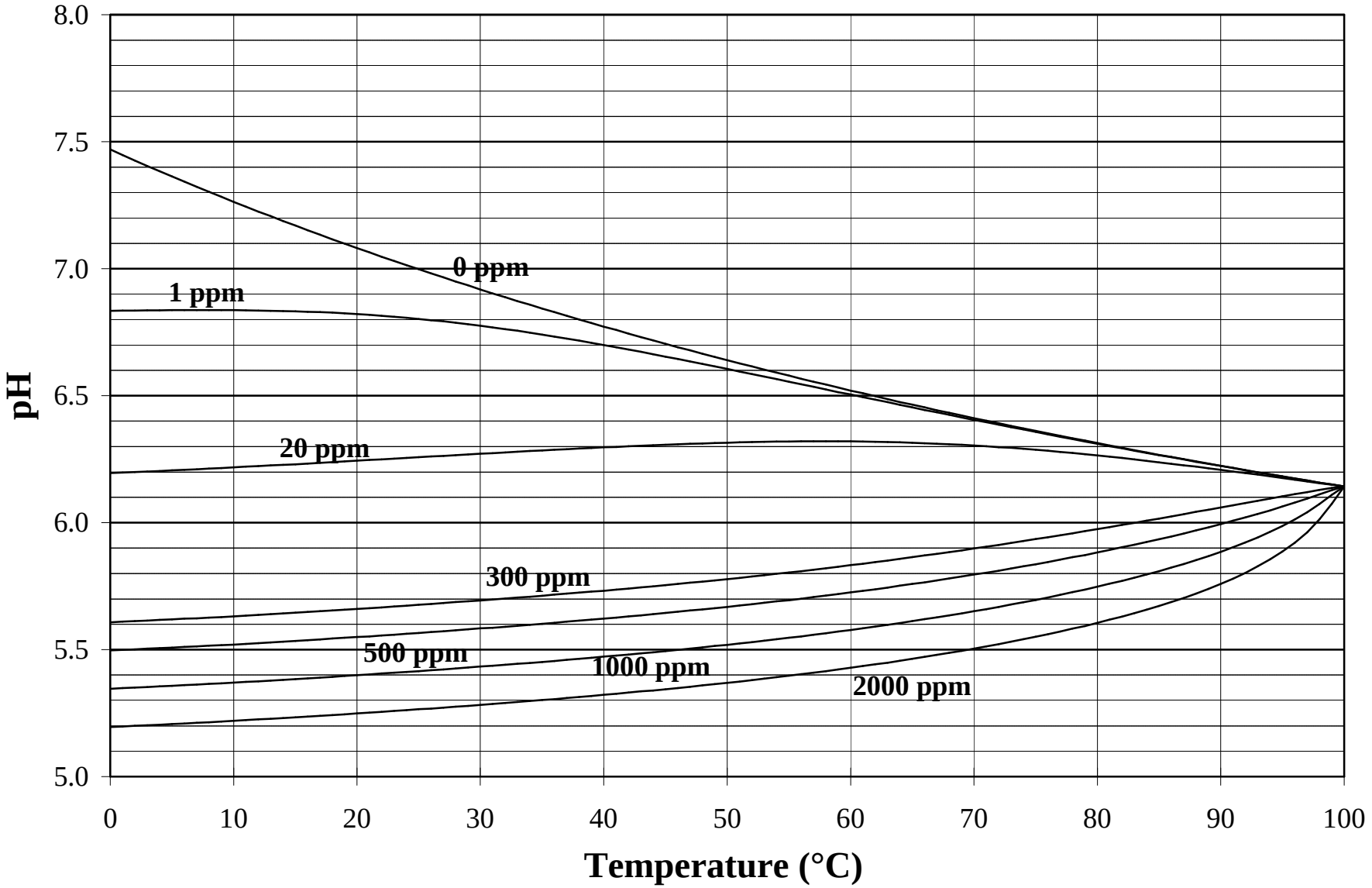

Table 1. Fundamental constants of CO_2/H_2O solutions

T (°C)	Exp. K_h (mol/L-atm)	Poly. K_h (mol/L-atm)	Rel. Error (%)	Exp. K_1 ($\times 10^{-7}$)	Poly. K_1 ($\times 10^{-7}$)	Rel. Error (%)	$K_W \acute{} 10^{-14}$ (molar)	$L°_{H^+}$ (S-cm^2/mol)	$L°_{OH^-}$ (S-cm^2/mol)	$L°_{HCO_3^-}$ (S-cm^2/mol)
0	0.0765	0.0764	0.08	2.64	2.67	-0.95	0.1152	225.04	118.35	22.3
5	0.0636	0.0636	-0.06	3.04	3.05	-0.29	0.1877	250.27	133.76	26.7
10	0.0533	0.0535	-0.27	3.44	3.44	0.14	0.2969	275.38	149.65	31.2
15	0.0455	0.0454	0.23	3.81	3.81	0.07	0.4573	300.29	165.92	35.6
20	0.0392	0.0390	0.53	4.16	4.15	0.23	0.6873	324.92	182.47	40.1
25	0.0339	0.0339	0.00	4.45	4.45	-0.07	1.010	349.19	199.24	44.5
30	0.0297	0.0298	-0.37	4.71	4.71	0.06	1.455	373.03	216.15	49.0
35	0.0264	0.0265	-0.11	4.90	4.91	-0.12	2.056	396.38	233.15	53.4
40	0.0237	0.0237	-0.12	5.04	5.05	-0.12	2.854	419.18	250.19	57.9
45	0.0214	0.0213	0.15	5.13	5.13	0.08	3.899	441.39	267.24	62.3
50	0.0195	0.0193	0.81	5.19	5.15	0.85	5.246	462.98	284.27	66.8
55		0.0175			5.11		6.957	483.90	301.26	71.2
60	0.0158	0.0158	-0.08		5.02		9.103	504.13	318.20	75.7
65		0.0142			4.87		11.76	523.67	335.11	80.1
70		0.0127			4.69		15.01	542.49	351.99	84.6
75		0.0111			4.46		18.93	560.60	368.88	89.0
80		0.0095			4.21		23.62	578.00	385.81	93.5
85		0.0077			3.94		29.17	594.71	402.82	97.9
90		0.0056			3.65		35.67	610.75	419.99	102.4
95		0.0030			3.36		43.21	626.14	437.37	106.8
100	0.0000	0.0000			3.07		51.90	640.92	455.05	111.3

Poly $K_h = -2.05\times10^{-11}T^5+6.40\times10^{-9}T^4-8.70\times10^{-7}T^3+6.44\times10^{-5}T^2-2.86\times10^{-3}T+7.64\times10^{-2}$

Poly $K_1 = -5.53\times10^{-17}T^5+2.39\times10^{-14}T^4-3.02\times10^{-12}T^3+4.71\times10^{-11}T^2+7.51\times10^{-9}T+2.67\times10^{-7}$

Table 2. Predicted conductivity of solutions exposed to low and ambient $CO_{2(g)}$ levels

T (°C)	0 ppm (mS/cm)	20 ppm (mS/cm)	300 ppm (mS/cm)	500 ppm (mS/cm)	1000 ppm (mS/cm)	2000 ppm (mS/cm)
0	0.0117	0.1579	0.6100	0.7875	1.1137	1.5749
5	0.0166	0.1727	0.6662	0.8600	1.2161	1.7197
10	0.0232	0.1863	0.7166	0.9250	1.3079	1.8495
15	0.0315	0.1986	0.7607	0.9817	1.3880	1.9627
20	0.0421	0.2098	0.7984	1.0302	1.4563	2.0591
25	0.0551	0.2203	0.8298	1.0704	1.5129	2.1389
30	0.0711	0.2304	0.8551	1.1025	1.5577	2.2019
35	0.0903	0.2408	0.8741	1.1262	1.5903	2.2474
40	0.1131	0.2519	0.8865	1.1410	1.6100	2.2742
45	0.1399	0.2647	0.8920	1.1464	1.6157	2.2810
50	0.1711	0.2801	0.8906	1.1420	1.6067	2.2663
55	0.2071	0.2994	0.8824	1.1276	1.5823	2.2289
60	0.2481	0.3237	0.8679	1.1035	1.5424	2.1683
65	0.2945	0.3544	0.8482	1.0704	1.4873	2.0844
70	0.3465	0.3923	0.8248	1.0296	1.4176	1.9773
75	0.4044	0.4380	0.8002	0.9828	1.3345	1.8472
80	0.4684	0.4920	0.7771	0.9324	1.2391	1.6938
85	0.5388	0.5542	0.7593	0.8815	1.1324	1.5155
90	0.6156	0.6246	0.7513	0.8345	1.0161	1.3081
95	0.6991	0.7030	0.7588	0.7986	0.8937	1.0628
100	0.7895	0.7895	0.7895	0.7895	0.7895	0.7895